

## Beauty baryons spectroscopy at LHCb

V. MATIUNIN(\*)

*Institute for Theoretical and Experimental Physics, NRC “Kurchatov Institute”  
Moscow, Russia*

received 16 September 2021

**Summary.** — A large dataset collected by the LHCb experiment in proton-proton collisions during Runs 1 and 2 of the Large Hadron Collider has opened a unique possibility to study beauty baryons and to broaden knowledge of their spectroscopy. Recent results on searches for new  $\Lambda_b^0$  baryon decays are reviewed. In particular, the observation of two new  $\Lambda_b^0 \rightarrow \psi(2S)p\pi^-$  and  $\Lambda_b^0 \rightarrow \chi_{c1}p\pi^-$  decays and the evidence for the  $\Lambda_b^0 \rightarrow \chi_{c2}p\pi^-$  decay are presented. Measurements of their branching fractions relative to that of the control channels are described.

### 1. – Introduction

The high energy of proton-proton (pp) collisions at the Large Hadron Collider (LHC) provides high production rate of b-quarks and access to the full range of b-hadrons including heavy  $\Lambda_b^0$  baryons. The excellent mass resolution, high efficiency of trigger and particle identification systems of the LHCb detector enable productive studies of many different  $\Lambda_b^0$  baryon decay channels, including multibody, rare, charmless and semileptonic decays. For example, in the amplitude analyses of the  $\Lambda_b^0 \rightarrow J/\psi pK^-$  decays a new class of baryonic resonances, hidden-charm pentaquarks, are observed in the  $J/\psi p$  system [1-3]. Also, evidence for contribution from the similar states are seen in the Cabibbo-suppressed decay  $\Lambda_b^0 \rightarrow J/\psi p\pi^-$  [4]. Recently, in the analysis of the  $\Xi_b^- \rightarrow J/\psi \Lambda K^-$  evidence for similar hidden-charm exotic states is seen in the  $J/\psi \Lambda$  system [5]. The charged charmonium-like tetraquark states  $Z_c^+$  are seen in the  $\chi_{c1}\pi^+$  and  $\psi(2S)\pi^+$  systems using the  $\bar{B}^0 \rightarrow \chi_{c1}\pi^+K^-$ ,  $\bar{B}^0 \rightarrow \psi(2S)\pi^+K^-$  and  $B^+ \rightarrow \psi(2S)\pi^+K_S^0$  decays [6-11]. Investigation of similar resonances, such as  $\psi(2S)p$ ,  $\chi_{c1}p$ ,  $\chi_{c2}p$ ,  $\psi(2S)\pi^-$ ,  $\chi_{c1}\pi^-$  and  $\chi_{c2}\pi^-$  with other b-decays modes could shed light on the nature of these exotic states. The decays  $\Lambda_b^0 \rightarrow \psi(2S)p\pi^-$ ,  $\Lambda_b^0 \rightarrow \chi_{c1}p\pi^-$  and  $\Lambda_b^0 \rightarrow \chi_{c2}p\pi^-$  provide an access to these two-particle systems, hence, are of particular interest.

The branching fractions of the decays  $\Lambda_b^0 \rightarrow \chi_{c2}pK^-$  and  $\Lambda_b^0 \rightarrow \chi_{c1}pK^-$  are measured to be almost equal [12]. This is very different from similar decays of B mesons where decays through  $\chi_{c2}$  mesons are significantly suppressed with respect to those through

(\*) E-mail: Viacheslav.Matiunin@cern.ch

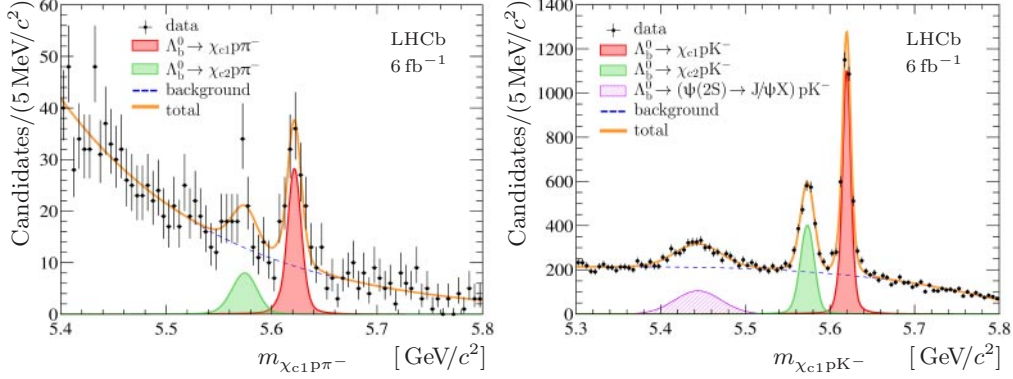


Fig. 1. – Mass distributions for selected (left)  $\Lambda_b^0 \rightarrow \chi_{cJ} p \pi^-$  and (right)  $\Lambda_b^0 \rightarrow \chi_{cJ} p K^-$  candidates. A fit, described in the text, is overlaid.

$\chi_{c1}$  mesons. Such suppression is in agreement with expectations from QCD factorisation [13]. More information about the b-baryon decays to the  $\chi_{c1}$  and  $\chi_{c2}$  states is needed to clarify the role of QCD factorisation in baryon decays.

In this paper, a search for the  $\Lambda_b^0 \rightarrow \chi_{c1} p \pi^-$ ,  $\Lambda_b^0 \rightarrow \chi_{c2} p \pi^-$  and  $\Lambda_b^0 \rightarrow \psi(2S) p \pi^-$  decays is reported. The  $\chi_{c1}$  and  $\chi_{c2}$  mesons are reconstructed using their radiative decays  $\chi_{cJ} \rightarrow J/\psi \gamma$ ,  $J/\psi$  and  $\psi(2S)$  mesons are reconstructed with the  $\mu^+ \mu^-$  final state. Throughout this paper the inclusion of charge-conjugated processes is implied and the symbol  $\chi_{cJ}$  is used to denote the  $\chi_{c1}$  and  $\chi_{c2}$  states collectively.

## 2. – Observation of the decay $\Lambda_b^0 \rightarrow \chi_{c1} p \pi^-$

The Cabibbo-suppressed decay  $\Lambda_b^0 \rightarrow \chi_{c1} p \pi^-$  is observed for the first time by the LHCb collaboration [14]. Also, evidence for the decay  $\Lambda_b^0 \rightarrow \chi_{c2} p \pi^-$  is found. The analysis is done using pp collision data sample corresponding to an integrated luminosity of  $6.0 \text{ fb}^{-1}$ , collected with the LHCb detector at a centre-of-mass energy of 13 TeV. As a normalisation channel the Cabibbo-favoured decay  $\Lambda_b^0 \rightarrow \chi_{c1} p K^-$  is used.

Similar selection criteria are applied to the channels under study, except for the requirements on pion candidates in the signal and kaon candidates in the normalisation channel. Selection criteria are based on the kinematics and topology parameters of the particles in the decay chain. Candidates used for the analysis satisfy trigger requirements based on the signal  $J/\psi$  candidates. The mass of the  $\Lambda_b^0$  candidates is calculated using a kinematic fit [15] to improve the  $\Lambda_b^0$  baryon mass resolution. In this fit, mass of the  $\mu^+ \mu^-$  combination is fixed to the nominal mass of the  $J/\psi$  meson and the mass of the  $J/\psi \gamma$  combination is fixed to the nominal mass of the  $\chi_{c1}$  meson. Thus, the  $\Lambda_b^0 \rightarrow \chi_{c1} p \pi^-$  and  $\Lambda_b^0 \rightarrow \chi_{c1} p K^-$  decays form a peak with the mean at the nominal mass of  $\Lambda_b^0$  baryon, whereas peaks from  $\Lambda_b^0 \rightarrow \chi_{c2} p \pi^-$  and  $\Lambda_b^0 \rightarrow \chi_{c2} p K^-$  decays are shifted towards the lower mass values [12, 16].

The mass spectra of the selected  $\Lambda_b^0 \rightarrow \chi_{cJ} p \pi^-$  and  $\Lambda_b^0 \rightarrow \chi_{cJ} p K^-$  candidates are shown in fig. 1. Signal yields are determined from unbinned extended maximum-likelihood fits to these distributions. The fit model consists of a signal contribution for each peak due to decay through  $\chi_{c1}$  and  $\chi_{c2}$  mesons and a combinatorial background component. In case of  $\Lambda_b^0 \rightarrow \chi_{cJ} p K^-$  candidates also a wide peaking component is used

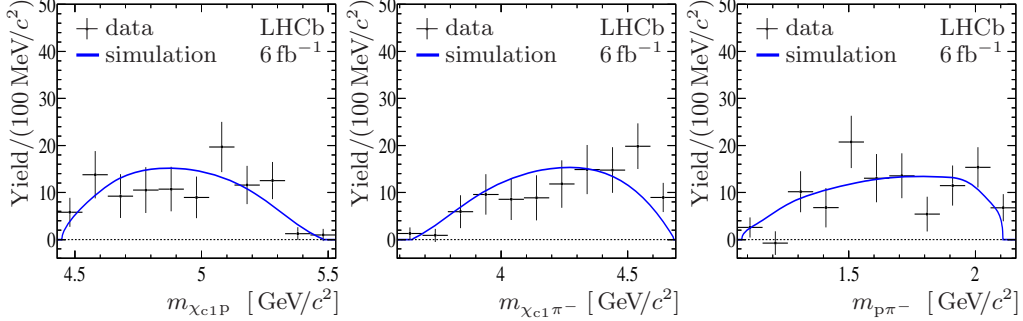


Fig. 2. – Background-subtracted mass distributions of the (left)  $\chi_{c1}p$ , (centre)  $\chi_{c1}\pi^-$  and (right)  $p\pi^-$  combinations in the  $\Lambda_b^0 \rightarrow \chi_{c1}p\pi^-$  decay. A phase-space simulation is overlaid.

in the fit model to account for partially reconstructed decays such as  $\Lambda_b^0 \rightarrow \psi(2S)pK^-$  with subsequent decays  $\psi(2S) \rightarrow J/\psi\pi\pi$ ,  $\psi(2S) \rightarrow J/\psi\eta$  or  $\psi(2S) \rightarrow (\chi_{c1} \rightarrow J/\psi\gamma)\gamma$ . Due to the low statistics in the  $\Lambda_b^0 \rightarrow \chi_{cJ}p\pi^-$  channels the difference in the mean values and the ratio of widths of the two peaks in the fit model for  $\Lambda_b^0 \rightarrow \chi_{cJ}p\pi^-$  candidates are constrained to the values obtained from simulation. The observed yields for the decays  $\Lambda_b^0 \rightarrow \chi_{c1}p\pi^-$ ,  $\Lambda_b^0 \rightarrow \chi_{c2}p\pi^-$ ,  $\Lambda_b^0 \rightarrow \chi_{c1}pK^-$  and  $\Lambda_b^0 \rightarrow \chi_{c2}pK^-$  are  $105 \pm 16$ ,  $51 \pm 16$ ,  $3133 \pm 75$  and  $1766 \pm 71$ , respectively. Statistical significance of the decays  $\Lambda_b^0 \rightarrow \chi_{c1}p\pi^-$  and  $\Lambda_b^0 \rightarrow \chi_{c2}p\pi^-$  is estimated using Wilks' theorem and found to be 9.6 and 3.8 standard deviations, respectively. Statistical significance of the  $\Lambda_b^0 \rightarrow \chi_{c2}p\pi^-$  decay is confirmed with simulation of large number of pseudoexperiments based on the background distributions observed in data.

Background-subtracted mass distributions of the  $\chi_{c1}p$ ,  $\chi_{c1}\pi^-$  and  $p\pi^-$  combinations in the  $\Lambda_b^0 \rightarrow \chi_{c1}p\pi^-$  decay are obtained using the *sPlot* technique [17] and are shown in fig. 2. The distributions from simulation, based on the phase-space decay model, are superimposed. With the current statistics no evidence for large contributions from possible exotic states is found.

Using the obtained signal yields the following branching fraction ratios are calculated:

$$\begin{aligned}
 (1a) \quad R_{\pi/K}^{\chi_{c1}} &\equiv \frac{\mathcal{B}(\Lambda_b^0 \rightarrow \chi_{c1}p\pi^-)}{\mathcal{B}(\Lambda_b^0 \rightarrow \chi_{c1}pK^-)} = \frac{N_{\Lambda_b^0 \rightarrow \chi_{c1}p\pi^-}}{N_{\Lambda_b^0 \rightarrow \chi_{c1}pK^-}} \times \frac{\varepsilon_{\Lambda_b^0 \rightarrow \chi_{c1}pK^-}}{\varepsilon_{\Lambda_b^0 \rightarrow \chi_{c1}p\pi^-}}, \\
 (1b) \quad R_{2/1}^{\pi} &\equiv \frac{\mathcal{B}(\Lambda_b^0 \rightarrow \chi_{c2}p\pi^-)}{\mathcal{B}(\Lambda_b^0 \rightarrow \chi_{c1}p\pi^-)} = \frac{N_{\Lambda_b^0 \rightarrow \chi_{c2}p\pi^-}}{N_{\Lambda_b^0 \rightarrow \chi_{c1}p\pi^-}} \times \frac{\varepsilon_{\Lambda_b^0 \rightarrow \chi_{c1}p\pi^-}}{\varepsilon_{\Lambda_b^0 \rightarrow \chi_{c2}p\pi^-}} \times R_{\chi_{c1}/\chi_{c2}}^{PDG}, \\
 (1c) \quad R_{2/1}^K &\equiv \frac{\mathcal{B}(\Lambda_b^0 \rightarrow \chi_{c2}pK^-)}{\mathcal{B}(\Lambda_b^0 \rightarrow \chi_{c1}pK^-)} = \frac{N_{\Lambda_b^0 \rightarrow \chi_{c2}pK^-}}{N_{\Lambda_b^0 \rightarrow \chi_{c1}pK^-}} \times \frac{\varepsilon_{\Lambda_b^0 \rightarrow \chi_{c1}pK^-}}{\varepsilon_{\Lambda_b^0 \rightarrow \chi_{c2}pK^-}} \times R_{\chi_{c1}/\chi_{c2}}^{PDG},
 \end{aligned}$$

where  $N$  is the measured yield,  $\varepsilon$  is the total efficiency of the corresponding decay and  $R_{\chi_{c1}/\chi_{c2}}^{PDG} \equiv \mathcal{B}(\chi_{c1} \rightarrow J/\psi\gamma)/\mathcal{B}(\chi_{c2} \rightarrow J/\psi\gamma)$  is the ratio of branching fractions of the radiative  $\chi_{cJ} \rightarrow J/\psi\gamma$  decays taken from PDG [18]. The total efficiency is determined as a product of the LHCb detector geometric acceptance, detection, reconstruction, selection and trigger efficiencies. Known differences between data and simulation are corrected

before calculating the efficiencies. In particular, for the simulation samples the combined detector response used for the particle identification is sampled using calibration data of high-statistics low-background decays  $D^{*+} \rightarrow (D^0 \rightarrow K^- \pi^+) \pi^+$ ,  $K_S^0 \rightarrow \pi^+ \pi^-$ ,  $D_s^+ \rightarrow (\phi \rightarrow K^+ K^-) \pi^+$ ,  $\Lambda \rightarrow p \pi^-$  and  $\Lambda_c^+ \rightarrow p K^- \pi^+$ .

Since the  $\Lambda_b^0 \rightarrow \chi_{cJ} p \pi^-$  and  $\Lambda_b^0 \rightarrow \chi_{cJ} p K^-$  decays have similar kinematics and topology most of the systematic uncertainties cancel in the ratios defined in eq. 1. For example, systematic uncertainties related to identification of muons and photons, reconstruction of  $J/\psi$  and  $\chi_{cJ}$  mesons are cancelled. The remaining contributions to the systematic uncertainties are studied. The largest contribution originates from the imperfect knowledge of signal and background shapes used for the fit of  $\Lambda_b^0$  baryon mass distributions. To estimate this contribution large number of high-statistics pseudoexperiments are generated with the baseline fit model and fitted using different alternative models. The maximal deviations of the yields ratios with respect to the baseline fit model are taken as a corresponding uncertainty of the  $R$  values. The other systematic uncertainties are related to the small discrepancy in the efficiency between data and simulation. Finally, uncertainty related to the finite size of the simulation sample is taken into account. Total systematic uncertainties calculated as a quadratic sum of partial components are 3.3, 3.8 and 3.8% for the  $R_{\pi/K}^{\chi_{c1}}$ ,  $R_{2/1}^\pi$  and  $R_{2/1}^K$  values, respectively. Also, for each alternative fit model, the statistical significance of the  $\Lambda_b^0 \rightarrow \chi_{c2} p \pi^-$  decay is estimated and the smallest value of 3.5 standard deviations is taken as a significance including systematic uncertainties.

Using the obtained yields and the calculated efficiencies ratios the branching fractions ratios are measured to be

$$(2a) \quad R_{\pi/K}^{\chi_{c1}} \equiv \frac{\mathcal{B}(\Lambda_b^0 \rightarrow \chi_{c1} p \pi^-)}{\mathcal{B}(\Lambda_b^0 \rightarrow \chi_{c1} p K^-)} = (6.59 \pm 1.01 \pm 0.22) \times 10^{-2},$$

$$(2b) \quad R_{2/1}^\pi \equiv \frac{\mathcal{B}(\Lambda_b^0 \rightarrow \chi_{c2} p \pi^-)}{\mathcal{B}(\Lambda_b^0 \rightarrow \chi_{c1} p \pi^-)} = 0.95 \pm 0.30 \pm 0.04 \pm 0.04,$$

$$(2c) \quad R_{2/1}^K \equiv \frac{\mathcal{B}(\Lambda_b^0 \rightarrow \chi_{c2} p K^-)}{\mathcal{B}(\Lambda_b^0 \rightarrow \chi_{c1} p K^-)} = 1.06 \pm 0.05 \pm 0.04 \pm 0.04,$$

where the first uncertainty is statistical, the second is systematic and the third is related to the uncertainties in the nominal branching fractions  $\mathcal{B}(\chi_{cJ} \rightarrow J/\psi \gamma)$  [18].

### 3. – Observation of the decay $\Lambda_b^0 \rightarrow \psi(2S) p \pi^-$

The  $\Lambda_b^0 \rightarrow \psi(2S) p \pi^-$  decay is observed for the first time by the LHCb collaboration [19]. The analysis is done using pp collision data sample corresponding to 1.0, 2.0 and  $1.9 \text{ fb}^{-1}$  of integrated luminosity, collected with the LHCb detector at a centre-of-mass energy of 7, 8 and 13 TeV, respectively. As a normalisation channel the Cabibbo-favoured decay  $\Lambda_b^0 \rightarrow \psi(2S) p K^-$  is used. The  $\psi(2S)$  mesons are reconstructed using the  $\mu^+ \mu^-$  final state.

Similar selection criteria are applied to both decay channels, except for the requirements on pion candidates in the signal and kaon candidates in the normalisation channel. Selection criteria are based on the kinematics and topology parameters of the particles in the decay chain. Candidates used for the analysis satisfy trigger requirements based on the signal  $\psi(2S)$  candidates. The mass of the  $\Lambda_b^0$  candidates is calculated using a kinematic fit [15] to improve the  $\Lambda_b^0$  baryon mass resolution. In this fit, mass of the  $\mu^+ \mu^-$  combination is fixed to the nominal mass of the  $\psi(2S)$  meson.

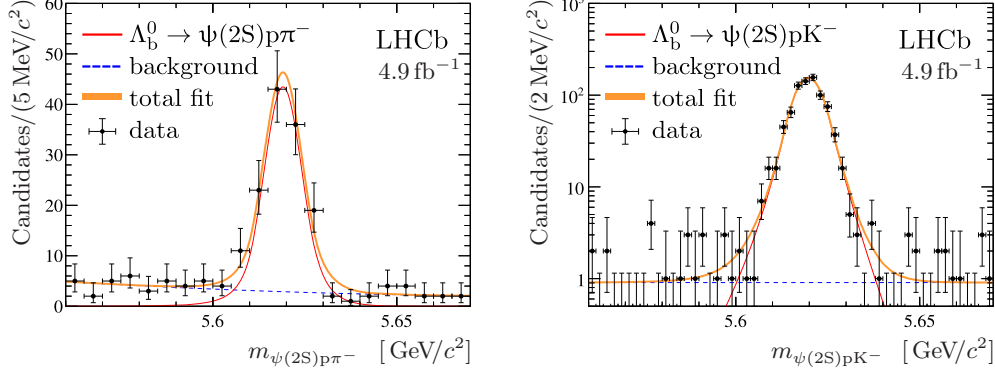


Fig. 3. – Mass distributions for selected (left)  $\Lambda_b^0 \rightarrow \psi(2S)p\pi^-$  and (right)  $\Lambda_b^0 \rightarrow \psi(2S)pK^-$  candidates. A fit, described in the text, is overlaid.

The mass spectra of the selected  $\Lambda_b^0 \rightarrow \psi(2S)p\pi^-$  and  $\Lambda_b^0 \rightarrow \psi(2S)pK^-$  candidates are shown in fig. 3. Signal yields are determined from unbinned extended maximum-likelihood fits to these distributions. The observed yields are  $121 \pm 13$  and  $806 \pm 29$  for the decays  $\Lambda_b^0 \rightarrow \psi(2S)p\pi^-$  and  $\Lambda_b^0 \rightarrow \psi(2S)pK^-$ , respectively. Statistical significance of the  $\Lambda_b^0 \rightarrow \psi(2S)p\pi^-$  decay is more than 9 standard deviations.

Background-subtracted mass distributions of the  $\psi(2S)p$ ,  $\psi(2S)\pi^-$  and  $p\pi^-$  combinations in the  $\Lambda_b^0 \rightarrow \psi(2S)p\pi^-$  decay are obtained using the *sPlot* technique [17] and are shown in fig. 4. The distributions from simulation, based on phase-space decay model, are superimposed. With the current statistics no evidence for large contributions from possible exotic states is found.

Using the obtained signal yields the following branching fraction ratios are calculated:

$$(3a) \quad R_{\pi/K}^\psi \equiv \frac{\mathcal{B}(\Lambda_b^0 \rightarrow \psi(2S)p\pi^-)}{\mathcal{B}(\Lambda_b^0 \rightarrow \psi(2S)pK^-)} = \frac{N_{\Lambda_b^0 \rightarrow \psi(2S)p\pi^-}}{N_{\Lambda_b^0 \rightarrow \psi(2S)pK^-}} \times \frac{\varepsilon_{\Lambda_b^0 \rightarrow \psi(2S)pK^-}}{\varepsilon_{\Lambda_b^0 \rightarrow \psi(2S)p\pi^-}},$$

where  $N$  is the measured yield,  $\varepsilon$  is the total efficiency of the corresponding decay.

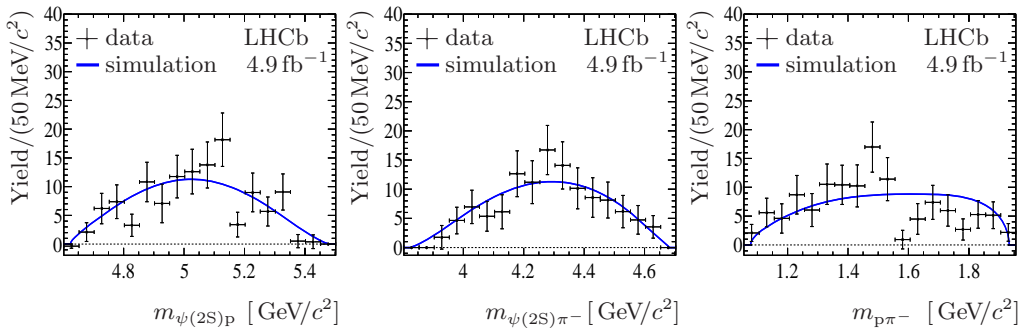


Fig. 4. – Background-subtracted mass distributions of the (left)  $\psi(2S)p$ , (centre)  $\psi(2S)\pi^-$  and (right)  $p\pi^-$  combinations in the  $\Lambda_b^0 \rightarrow \psi(2S)p\pi^-$  decay. A phase-space simulation is overlaid.

The total efficiency is determined as a product of the LHCb detector geometric acceptance, detection, reconstruction, selection and trigger efficiencies. Efficiencies of particle identification are calculated using calibration data samples of high-statistics low-background decays  $D^{*+} \rightarrow (D^0 \rightarrow K^- \pi^+) \pi^+$ ,  $K_S^0 \rightarrow \pi^+ \pi^-$ ,  $D_s^+ \rightarrow (\phi \rightarrow K^+ K^-) \pi^+$ ,  $\Lambda \rightarrow p \pi^-$  and  $\Lambda_c^+ \rightarrow p K^- \pi^+$ . Each of the other partial efficiencies is calculated using the simulation samples appropriately corrected for the known differences between data and simulation.

Since the  $\Lambda_b^0 \rightarrow \psi(2S)p\pi^-$  and  $\Lambda_b^0 \rightarrow \psi(2S)pK^-$  decays have similar kinematics and topology most of the systematic uncertainties cancel in the ratios defined in eq. 3. For example, systematic uncertainties related to identification of muons and reconstruction of  $J/\psi$  mesons are cancelled. The remaining contributions to the systematic uncertainties are studied. The largest contribution originates from the discrepancy in trigger efficiency between data and simulation. This effect has been previously studied by comparing ratios of trigger efficiencies in data and simulation for the high-yield  $B^+ \rightarrow J/\psi K^+$  and  $B^+ \rightarrow \psi(2S)K^+$  decays [20]. The rest of the systematic uncertainties are related to the small discrepancy in the other partial efficiencies between data and simulation. Finally, the uncertainty related to the choice of the fit model and the uncertainty due to the finite size of the simulation sample are taken into account. Total systematic uncertainty calculated as a quadratic sum of partial components is 1.7%.

Using the obtained yields and the calculated efficiencies ratio the branching fractions ratio is measured to be

$$(4a) \quad R_{\pi/K}^{\psi} \equiv \frac{\mathcal{B}(\Lambda_b^0 \rightarrow \psi(2S)p\pi^-)}{\mathcal{B}(\Lambda_b^0 \rightarrow \psi(2S)pK^-)} = (11.4 \pm 1.3 \pm 0.2) \times 10^{-2},$$

where the first uncertainty is statistical, the second is systematic.

#### 4. – Comparison with analogous previous measurements

The measured  $R_{\pi/K}^{\chi_{c1}}$  and  $R_{\pi/K}^{\psi}$  ratios are compared with previous analogous measurements. The branching fraction ratio between Cabibbo-suppressed and Cabibbo-favoured decays are defined as

$$(5a) \quad R \equiv \frac{\mathcal{B}(\text{suppressed})}{\mathcal{B}(\text{favoured})}.$$

The phase-space corrected ratios are defined as

$$(6a) \quad R^{\Phi} \equiv \frac{\mathcal{B}(\text{suppressed})}{\mathcal{B}(\text{favoured})} \times \frac{\Phi(\text{favoured})}{\Phi(\text{suppressed})},$$

where  $\Phi$  stands for either two- or three-body phase-space. For three-body decays phase-space is calculated neglecting possible intermediate resonances. The ratios  $R$  and  $R^{\Phi}$  are shown in fig. 5. Given that resonance structure is not taken into account for the three-body decays, even  $R^{\Phi}$  ratios are not expected to be exactly the same. The ratios are distributed around Cabibbo-suppression factor of  $\sim 5\%$  and the new measurements follow the same tendency.

Measurement of the  $R_{2/1}^K$  ratio is in agreement with the previous LHCb measurement of  $1.02 \pm 0.11$  [12]. The new result has better precision and is obtained using a data

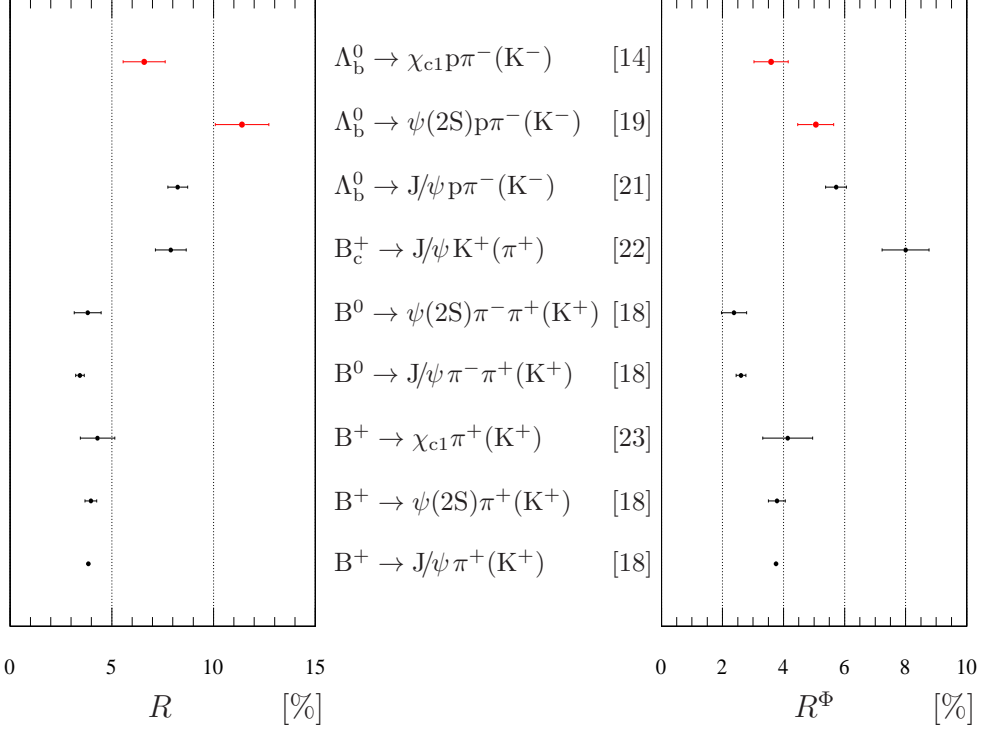


Fig. 5. – The ratios  $R$  and  $R^\Phi$  for the selected two- and three-body decays of beauty hadrons.

sample statistically independent from the one used for the previous measurement. The measured  $R_{2/1}^\pi$  ratio also shows no suppression of the  $\chi_{c2}$  mode with respect to the  $\chi_{c1}$  mode and the result is in agreement with the  $R_{2/1}^K$  value.

## 5. – Conclusion

Using proton-proton collision data samples collected by the LHCb experiment at a centre-of-mass energies of 7, 8 and 13 TeV the decays  $\Lambda_b^0 \rightarrow \psi(2S) p \pi^-$  and  $\Lambda_b^0 \rightarrow \chi_{c1} p \pi^-$  are observed for the first time. Also, evidence for the  $\Lambda_b^0 \rightarrow \chi_{c2} p \pi^-$  decay is found. Branching fractions of the  $\Lambda_b^0 \rightarrow \psi(2S) p \pi^-$  and  $\Lambda_b^0 \rightarrow \chi_{c1} p \pi^-$  decays are measured relative to that of the  $\Lambda_b^0 \rightarrow \psi(2S) p K^-$  and  $\Lambda_b^0 \rightarrow \chi_{c1} p K^-$  decays, respectively. The measured branching fraction ratios are in agreement with the analogous previous measurements. The measurements of the  $R_{2/1}^\pi$  and  $R_{2/1}^K$  ratios show no suppression of the  $\chi_{c2}$  mode relative to the  $\chi_{c1}$  mode for both  $\Lambda_b^0 \rightarrow \chi_{cJ} p \pi^-$  and  $\Lambda_b^0 \rightarrow \chi_{cJ} p K^-$  cases, which challenges the factorisation approach for the  $\Lambda_b^0$  baryon decays [13]. The background-subtracted mass spectra of  $\psi(2S) p$  and  $\psi(2S) \pi^-$  combinations in the  $\Lambda_b^0 \rightarrow \psi(2S) p \pi^-$  decay and  $\chi_{c1} p$  and  $\chi_{c1} \pi^-$  combinations in the  $\Lambda_b^0 \rightarrow \chi_{c1} p \pi^-$  decay are investigated and no evidence for contributions from exotic states is found.

\* \* \*

This work is supported by the Russian Foundation for Basic Research under grant No. 20-32-90166. Also, the author would like to express special thanks to the La Thuile 2021 organizers for the great virtual conference.

## REFERENCES

- [1] LHCb COLLABORATION (AAIJ R. *et al.*), *Phys. Rev. Lett.*, **115** (2015) 072001.
- [2] LHCb COLLABORATION (AAIJ R. *et al.*), *Phys. Rev. Lett.*, **117** (2016) 082002.
- [3] LHCb COLLABORATION (AAIJ R. *et al.*), *Phys. Rev. Lett.*, **122** (2019) 222001.
- [4] LHCb COLLABORATION (AAIJ R. *et al.*), *Phys. Rev. Lett.*, **117** (2016) 082003.
- [5] LHCb COLLABORATION (AAIJ R. *et al.*), to be published in *Science Bulletin*, arXiv:2012.10380.
- [6] BELLE COLLABORATION (CHOI S.-K. *et al.*), *Phys. Rev. Lett.*, **100** (2008) 142001.
- [7] BELLE COLLABORATION (MIZUK R. *et al.*), *Phys. Rev. D*, **80** (2009) 031104.
- [8] BELLE COLLABORATION (CHILIKIN K. *et al.*), *Phys. Rev. D*, **88** (2013) 074026.
- [9] LHCb COLLABORATION (AAIJ R. *et al.*), *Phys. Rev. Lett.*, **112** (2014) 222002.
- [10] LHCb COLLABORATION (AAIJ R. *et al.*), *Phys. Rev. D*, **92** (2015) 112009.
- [11] BELLE COLLABORATION (MIZUK R. *et al.*), *Phys. Rev. D*, **78** (2008) 072004.
- [12] LHCb COLLABORATION (AAIJ R. *et al.*), *Phys. Rev. Lett.*, **119** (2017) 062001.
- [13] BENEKE M. and VERNAZZA L., *Nucl. Phys. B*, **811** (2009) 155.
- [14] LHCb COLLABORATION (AAIJ R. *et al.*), *JHEP*, **05** (2021) 095.
- [15] HULSBERGEN W. D., *Nucl. Instrum. Methods A*, **552** (2005) 566.
- [16] LHCb COLLABORATION (AAIJ R. *et al.*), *Nucl. Phys. B*, **874** (2013) 663.
- [17] PIVK M. and LE DIBERDER F. R., *Nucl. Instrum. Methods A*, **555** (2005) 356.
- [18] PARTICLE DATA GROUP (ZYLA P. A. *et al.*), *Prog. Theor. Exp. Phys.*, **2020** (2020) 083C01.
- [19] LHCb COLLABORATION (AAIJ R. *et al.*), *JHEP*, **08** (2018) 131.
- [20] LHCb COLLABORATION (AAIJ R. *et al.*), *Eur. Phys. J. C*, **72** (2012) 2118.
- [21] LHCb COLLABORATION (AAIJ R. *et al.*), *JHEP*, **07** (2014) 103.
- [22] LHCb COLLABORATION (AAIJ R. *et al.*), *JHEP*, **09** (2016) 153.
- [23] BELLE COLLABORATION (KUMAR R. *et al.*), *Phys. Rev. D*, **74** (2006) 051103.